Ab initio atomistic thermodynamics modeling of adsorption of oxygen on gold and gold-silver surfaces

Mehmet Gökhan ŞENSOY[*]

Department of Physics, Faculty of Science, Recep Tayyip Erdoğan University, Rize, Turkey

Abstract: A theoretical study of oxygen adsorption on gold and gold-silver surfaces by means of density functional theory (DFT) calculations with an atomistic thermodynamic model is performed. The (111) and (211) facets of gold and gold-silver alloy surfaces are considered, and their stabilization is discussed upon adsorption of oxygen depending on O and Ag coverage. The details of how the DFT-based atomistic thermodynamic model can apply to the transition metal surface are also presented in this work.

Key words: Density functional theory, atomistic thermodynamics model, oxidation, transition metal surfaces

1. Introduction

Activation of molecular oxygen is a critical step in heterogeneous catalysis, and the interaction of the molecular oxygen with the metal surface affects the stability and reactivity of the catalyst [1–9]. These are important for the oxidative chemistry and play important roles in the global economy. The main issue is understanding and predicting oxidation catalysis in O_2 activation on transition metal surfaces in heterogeneous catalysis processes [9]. Methoxy and formaldehyde production from methanol [10], CO oxidation [11], ethylene epoxidation [12], and hydrocarbon conversion [13] in catalytic converters can be given as examples for the important catalytic processes including O_2 activation on transition metals.

Another important point in the activation of molecular oxygen is that charge transfer from metal surfaces to the stable oxygen molecule becomes more reactive, yielding CO, for example, and lowers the dissociation barrier of O_2 [9, 14]. This energy barrier depends on the electronic and geometric structure of the metal surface. For this reason the prediction of the surface structure for the active oxygen on the surface is the key step in surface science since the surface O reacts with surface molecules (such as CO, methanol, and methoxy) in catalytic reactions. To understand the catalytic function of the metal surfaces, the knowledge of oxidation properties of transition metal surfaces is important. In particular, the surface properties can change under oxidation reaction conditions and show different reactivity and selectivity.

With the discovery of catalytic activity of gold, there is rapid increase in the number of Au-based catalysts for the industrially important chemical processes mentioned above. Research on Au-based catalysts has gained momentum due both to their activity and selectivity at low temperatures and their low environmental impact. Meanwhile, studies on gold-based catalysis have been extended to gold alloys with Ag or Cu [15, 16]. Recent works showed that Ag can be used to manipulate the catalytic properties by varying particle size and

*Correspondence: mehmet.sensoy@erdogan.edu.tr

chemical composition [16, 17]. The Ag content increases the catalytic activity and selectivity in oxidation reactions [14, 16, 18, 19]. For example, the step sites of Ag-Au alloy can dissociate O_2 with the help of Ag atoms [19–21], while Au step sites cannot dissociate according to previous studies [22, 23].

Adsorbed O with other reactive species act as initiators for many reaction steps on Au and Ag surfaces. Experimental studies have indicated that Au and Ag surfaces pretreated with atomic oxygen successfully catalyze selective oxidation [24–26]. The catalysts used in these experiments include clean oxygen pretreated [24–26], reconstructed [27, 28], and defective [27, 28] Au and Ag surfaces. Surface oxidizing species such as O, OH, and CH_3O are needed for reaction to occur on the surface, and the site where they react with surface intermediates will be the active site. Moreover, chemisorbed O has a crucial role in the stabilization of surface water and the formation of hydroxyl groups on the surface [29, 30]. Though there exist theoretical studies on the structural and electronic properties of oxide transition metal surfaces [31–33], there are very few comparable and complete studies on the thermodynamic properties. Also, a detailed study of how the DFT-based atomistic thermodynamic model can apply to the transition metal surfaces including bimetallic surfaces is absent. For these reasons, we have theoretically studied the surface stability of the flat and step surfaces of Au with Ag-Au bimetallic surfaces and compared that with experimental results.

In this study, we present the details of DFT-based atomistic thermodynamic modeling for metal surfaces. Then we report on the thermodynamic stability by using an ab initio atomistic thermodynamics method [31, 33–37] of on-surface oxygen on flat and step Au and Ag-Au surfaces as a function of temperature and partial pressure of O_2 as well as change of their properties in the presence of Ag.

2. Method

2.1. Computational details

All DFT calculations in the present work are performed using the Vienna Ab initio simulation package (VASP) [38, 39] with the GGA-PBE [40] functional to describe electron exchange and correlation. We employ the projector-augmented wave method [41, 42] with a plane-wave basis set (cutoff = 400 eV). For the Brillouin zone integrations, we use a Γ-centered $7 \times 7 \times 1$ Monkhorst-Pack k-point grid [43]. The (111) and (211) surfaces are modeled by a four-layer slab with a vacuum of 13 Å between slabs. Tkatchenko–Scheffler correction [44] is used for van der Waals interactions. Spin polarization is not employed since the effect of polarization was found to be negligible during preliminary tests. Adsorption energies of oxygen on the surface are obtained as follows:

$$E_{\text{ads}} = E_{\text{total}} - E_{\text{surface}} - E_{\text{oxygen}}, \tag{1}$$

where E_{total}, E_{surface}, and E_{oxygen} are the total energy of the structure, the energy of the pristine surface (without any adsorbate), and the energy of the oxygen atom in the gas phase, respectively.

2.2. Atomistic thermodynamic model

DFT has become a standard tool for electronic structure calculations to understand the ground state properties at 0 K, and using the DFT results can provide detailed information in the microscopic regime. The results from DFT are then combined with the concepts of thermodynamic and statistical mechanics to get the material properties in meso- and macroscopic regime. In results from the electronic structure calculations the temperature (T) and pressure (P) effects on the material properties are not included as the obtained physical quantities are

only valid at 0 K and zero pressure. For this reason, to describe the situations of a considered system under temperature and pressure, the DFT results can be used for the thermodynamic considerations [19, 33, 45].

To describe the considered system under oxidation conditions at a finite temperature and pressure, the results from DFT calculations can be used as input. Then the related thermodynamic functions can be evaluated over the temperature and pressure range [45]. Here, the key quantity is the Gibbs free energy, G:

$$G(T,p) = E_{tot} + F_{vib} - TS_{conf} + PV, \tag{2}$$

where E_{tot} is the total energy obtained from electronic calculations, $F_{vib} = E_{ZPE}$ - TS_{vib} is the vibrational free energy, S_{conf} is the configurational entropy, and the last term is the product of pressure and volume. If the considered system is in thermodynamic equilibrium, the DFT and the thermodynamics can be applicable to the system. Another important point is that if the system is in thermodynamic equilibrium, the system can be divided into smaller subsystems, which are in thermodynamic equilibrium with each other (see Figure 1). Therefore, each subsystem can be treated separately within DFT. Such atomistic thermodynamics can be used to calculate the surface free energy and once for the Gibbs free energy of adsorption.

For a system in thermodynamic equilibrium, one component of the system can be described with thermodynamic quantities of internal energy (E), entropy (S), volume (V), the number of particles (N), and the chemical potential (μ) in the system as:

$$E_{bulk} = TS - PV + N\mu. \tag{3}$$

If a homogeneous bulk material is cleaved, two surfaces with surface area of A are created by increasing the internal energy of the system proportional to the surface area. The constant of proportionality can be defined as the surface energy [46], γ, and the surface energy cleaved from the bulk can be written as:

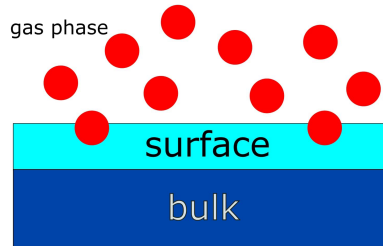$$E_{bulk} = TS - PV + N\mu + \gamma A. \tag{4}$$

Figure 1. Surface in thermodynamic equilibrium. The system can be divided into subsystems in thermodynamic equilibrium as bulk, surface, and gas phase. The energetics of them can be treated separately from the DFT calculations.

Introducing the Gibbs free energy in Eq. (2.2), the surface free energy in more general form is defined as:

$$\gamma = \frac{1}{A}[G_{surf} - \sum_i N_i \mu_i(T, P_i)], \tag{5}$$

where G_{surf} is the Gibbs free energy of cleaved bulk structure, and $\mu_i(T, P_i)$ is the chemical potential of the various species (i) in the system. In the case of the metal-oxide system the surface free energies will be investigated as a function of chemical potential of metal and oxygen. For this reason, the surface free energy, γ, in Eq. (2.5) can be modified as follows:

$$\gamma = \frac{1}{A}[G_{surf} - N_m \mu_m(T, P) - N_O \mu_O(T, P)], \tag{6}$$

where N_m and N_O are the number of metal and oxygen atoms in the system, μ_m and μ_O are the chemical potentials of metal and oxygen atoms, and A is the surface area. In previous works [36, 45], it was shown that the vibrational and entropy contributions have small contributions and these quantities do not vary so much for different surface configurations. From a simple dimensional analysis for the PV, its contribution to the surface free energy per surface area (PV/A) will be 10^{-3} meV/A^2 at 1 atm. For the vibrational contribution, it was reported that the F_{vib} value stays within ~ 5 meV/A^2 for the entire temperature rate up to 600 K according to the variations of the characteristic vibrational modes [31]. Therefore, the Gibbs energy, G_{surf}, can be approximately obtained from the DFT total energy.

If the considered system is a bimetallic system, the calculation of chemical potentials of metal atoms will be complicated. To calculate the chemical potentials, we assume that the surface is in thermodynamic equilibrium with a dilute metal bulk alloy (mn, $N_m = 1$, $N_n = N_{mn} - N_m$) and a reservoir of molecular oxygen. Then the chemical potentials of metals m and n can be calculated by using the total energies of the bulk structures as follows:

$$\mu_n = E_n^{bulk(n)}/N_n^{bulk(n)}, \tag{7}$$

$$\mu_m = [E_{mn}^{bulk(mn)} - N_n^{bulk(mn)}\mu_n]/N_m^{bulk(mn)}. \tag{8}$$

The chemical potential of molecular oxygen as a function of temperature and pressure is given by:

$$\mu_O(T, P) = \frac{1}{2}\big(E_{O_2} + \Delta\mu_{O_2}(T, P)\big), \tag{9}$$

where E_{O_2} is the O$_2$ energy in gas phase. For the total energy of the molecular oxygen O$_2$, we have used the corrected energy obtained from the experimental heat formation energy of water ($\Delta_f H_{0,H_2O}$) as:

$$E_{O_2}^{gas} = 2(E_{H_2O}^{gas} - E_{H_2}^{gas} + \Delta ZPE + \Delta_f H_{0,H_2O}). \tag{10}$$

The relative chemical potential of oxygen, $\Delta\mu_{O_2}(T, P)$, is defined as:

$$\Delta\mu_{O_2}(T, P) = \mu_{O_2}(T, P^0) + k_\beta T \ln(P/P^0), \tag{11}$$

where P^0 is the atmospheric pressure (~ 1 atm) and the $\mu_{O_2}(T, P^0)$ is the thermodynamic function of O_2. We use tabulated enthalpy and entropy values to calculate $\Delta\mu_{O_2}$, as done in previous work [31]. Here, the zero-point vibrational energy term (ΔZPE) was not considered due to its small energy contribution (~ 20 meV).

3. Results

3.1. Ag(111) and Au(111) surfaces

We begin our study on the stability of adsorbed oxygen by examining oxygen on the Ag(111) and Au(111) surfaces. According to the calculated adsorption energies (see Figure 2) for the considered surfaces, the O on Ag(111) is found more stable than the Au(111) surface at different surface O coverages. However, the fully Ag covered Ag/Au(111) surface is the most favorable one due to the Ag-Au interatomic interaction introducing an extra stabilization. To understand the effect of the temperature and pressure on the structure stability, we include a wide variety of structures in the calculations for the (111) surfaces of Ag and Au, and the surface free energies are calculated for the most stable O coverage configurations with respect to the relative O chemical potential. The most thermodynamically favorable O coverage at a given O chemical potential difference (or corresponding temperature) is one of the lowest values of surface free energy.
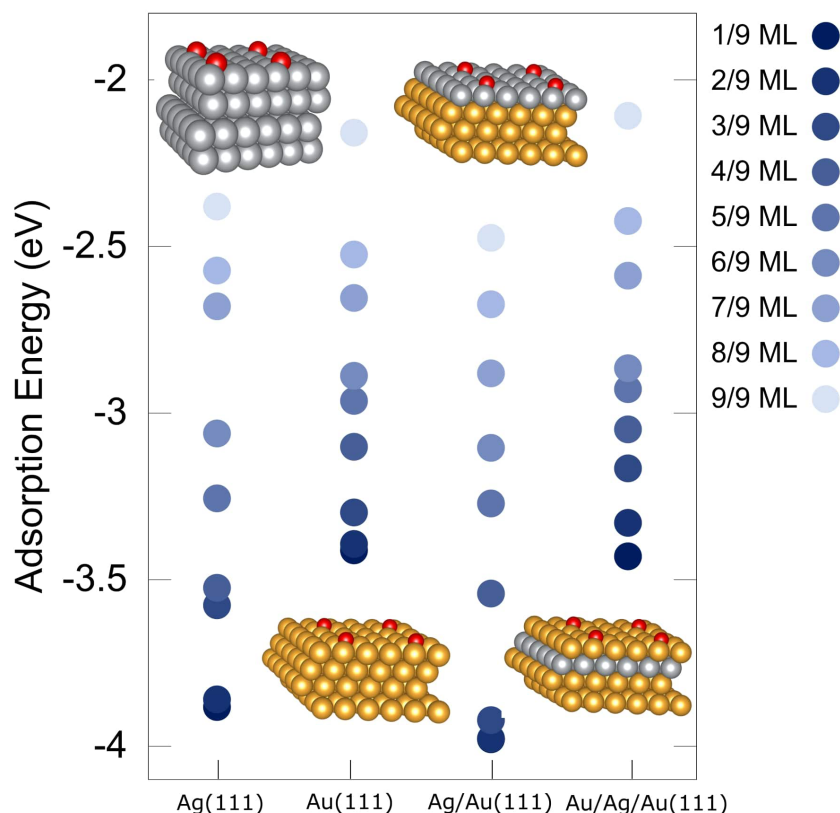

Figure 2. Adsorption energies of oxygen on Ag(111), Au(111), Ag/Au(111), and Au/Ag/Au(111) surfaces. The surface structures for 1/9 ML O coverage are given as inset figures. Gray, gold, and red balls stand for Ag, Au, and O, respectively.

To identify which surface coverage is most thermodynamically stable for a certain temperature and the partial O_2 pressure ($P_{O_2} = 1$, 10^{-3}, and 10^{-12} atm), the surface free energies are plotted in Figures 3a–3c for the most favorable configurations at the coverage of 1/9–9/9 monolayers (ML, number of adsorbates per number of surface metal atoms) O on Ag(111). The 2/9 ML O coverage having the lowest surface free energy in the phase diagram is the most stable, and surface structures lower than 4/9 ML O coverage are found to be
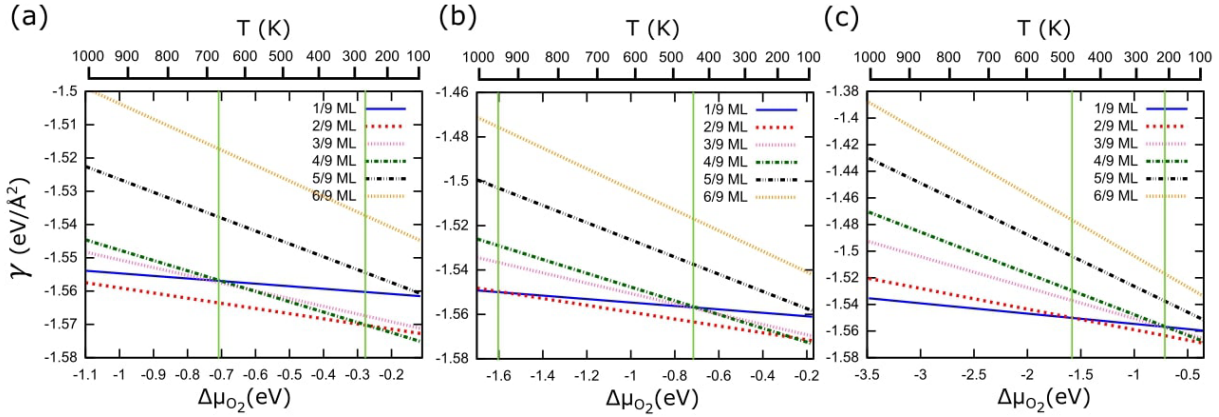
Figure 3. Surface free energy (γ) as a function of the chemical potential of oxygen (μ_{O_2}) for different on-surface O coverage depending on the temperature at a fixed partial pressure of O_2, (a) $P_{O_2} = 1$, (b) 10^{-3}, and (c) 10^{-12} atm (or equivalently the corresponding temperature values at a fixed O_2 pressure) on Ag(111) surface. The green vertical lines stand for the phase transition.

thermodynamically most stable at lower temperatures (<400 K). When the partial pressure of O_2 increases, the 1/9 ML coverage becomes the most favorable; see Figures 3b and 3c. In the work of Li et al. [33], it was reported that the 1/4 ML O coverage is the most stable at higher temperatures, and this result is consistent with our findings. They also reported that very low concentration of the chemisorbed O on the surface are stable at higher temperatures, and so it can play a role in oxidation reactions at high temperature. As expected from the thermodynamic considerations, the lower O_2 partial pressure (10^{-12} atm) and/or higher temperatures are favorable for the lower oxygen coverages on Ag(111). At the same time, the most stable phases due to the stronger adsorption of oxygen corresponding to regular chemisorption of O, 1/9, and 2/9 ML O coverages appear in Figures 3b and 3c at partial pressures of $P_{O_2} = 10^{-3}$ and 10^{-12} atm.

Now we address the question of whether surface O can be stabilized by Ag content in the (111) surface of Au. In the case of O adsorption on the Au(111) surface, we have prepared three different surface configurations to understand the Ag effect on the stabilization of O. These are labeled as Au(111), Ag/Au(111), and Au/Ag/Au(111) and are presented in Figure 2.

According to the calculated adsorption energies of O on the surfaces in Figure 2, the most favorable surface is the fully Ag covered (top-most layer) Ag/Au(111) surface, and the O energies are nearly the same for the Au(111) and Au/Ag/Au(111) surfaces. This can be easily seen from the surface free energy plots in Figures 4a–4c for the surfaces. The surface free energy profiles are nearly the same for the Au(111) and Au/Ag/Au(111) surfaces as seen in Figures 4a and 4c. The most favorable O coverage is found as the 0.11 and 2/9 ML O coverage on the Au(111) and Au/Ag/Au(111) surfaces at fixed partial pressure of O, 1, 10^{-3}, and 10^{-12} atm. Under ultrahigh vacuum (UHV) conditions, $P_{O_2} = 10^{-12}$ atm, the 1/9 ML O coverage is the most favorable chemisorbed O, which is strongly bound to the surface with the value of adsorption energy greater than –3.5 eV configuration at all temperature ranges. For the Ag/Au(111) surface, the 3/9 ML O coverage is the most favorable at $P_{O_2} = 1$ atm. However, under UHV conditions, the 1/9 ML O coverage is found to be the most stable at temperatures higher than 500 K, and the 3/9 ML O coverage is still more favorable at lower temperatures.
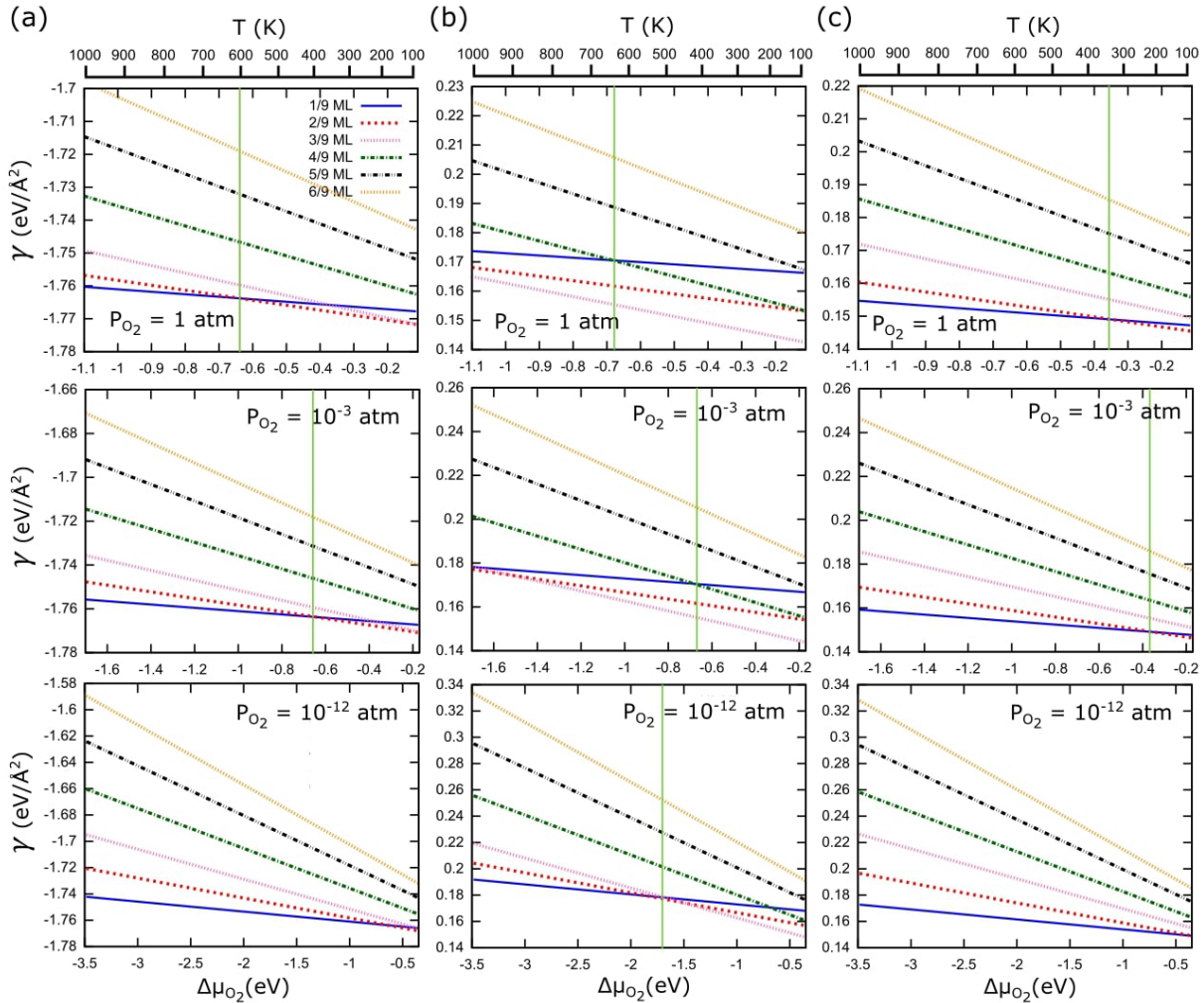
Figure 4. Surface free energy (γ) as a function of the chemical potential of oxygen (μ_{O_2}) for different on-surface O coverage depending on the temperature at a fixed partial pressure of O_2, $P_{O_2} = 1$, 10^{-3}, and 10^{-12} atm (or equivalently the corresponding temperature values at a fixed O_2 pressure) on (a) Au(111), (b) Ag/Au(111), and (c)Au/Ag/Au(111) surfaces. The green vertical lines stand for the phase transition.

3.2. Au(211) and AgAu(211) surfaces

Results from previous studies [19, 47] showed that the dissociation of oxygen molecules is easier on the step surface of Au(211) than the flat Au(111) surface. For this reason, understanding the effect of the step surface on the stabilization of oxygen becomes important. Besides this, the Ag content of the Au(211) surface can increase the dissociation probability on the surface, increasing the surface activity [19]. In this part of the study, we first investigate the thermodynamic stability of surface O coverage in Au(211) and dilute AgAu(211) surfaces, and then work on the effect of the Ag content in the stabilization of the O adsorption under thermodynamic conditions. In the AgAu(211) surface, all surface step atoms are replaced with Ag atoms, resulting in Ag surface coverage (Θ_{Ag}) of 6/9 ML. We have found that the O atoms are more stable on the step surface than the flat surface of Au (0.14 eV stronger), and an additional 0.28 eV more strongly on AgAu(211) than Au(211) surface. The adsorption energies are presented in Figure 5 for different on-surface O coverages in a range between 1/9 and 6/9 ML O.
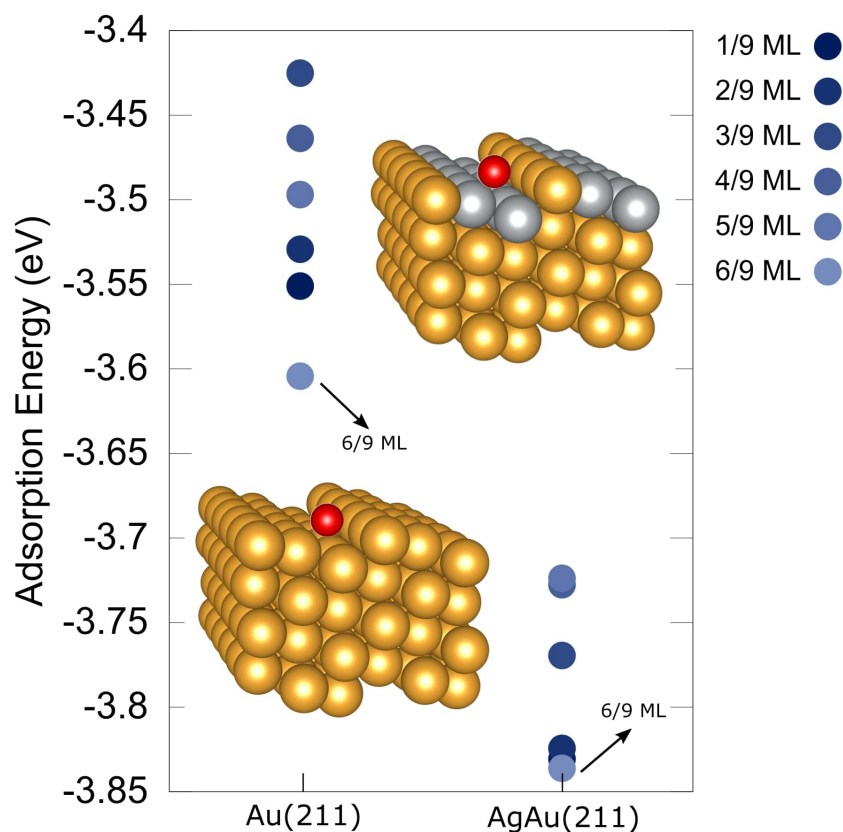
Figure 5. Adsorption energies of oxygen on Au(211) and AgAu(211) surfaces. The surface structures for 1/9 ML O coverage are given as inset figures. Gray, gold, and red balls stand for Ag, Au, and O, respectively.

The surface free energies for the 1/9–6/9 ML O coverages on Au(211) and AgAu(211) surfaces are given in Figure 6. Our results show that the most favorable O coverage is 6/9 ML on both surfaces incorporating the most stable O-Au-O atomic arrangement at the partial pressure of O_2 1 atm. Under UHV conditions, the 1/9 ML O coverage becomes more favorable at temperatures higher than 370 K for the Au(211) and higher than 480 K for the AgAu(211) surface. At 10^{-3} atm, the 1/9 ML O coverage on Au(211) becomes more stable than the 6/9 ML at higher temperatures. In previous studies, the higher O coverage at 400 K is found to be stable and the formation of chemisorbed surface O was seen due to the porous structure of the surface [32, 48]. The thermodynamic stability and also the surface O coverage becomes critical in determining the selectivity of Au and AuAg surfaces in oxidation catalysis [49]. It is reported that the partial pressure of O_2 can affect the selectivity of the Au and AuAg alloy surfaces. Our results are consistent with these results and support the experimental results in the study of Wittstock et al. [49].

Our results also show that the AuAg surfaces have chemisorbed surface O under experimental reaction conditions [50], at 423 K and 5×10^{-2} atm, and the thermodynamic stability of surface O depends on the Ag concentration on the surfaces [49].

To understand which surface O coverage is most thermodynamically stable for a given temperature and Ag coverage, we have calculated the surface free energies for the most stable adsorption configurations at O coverage of 1/9, 2/9, 3/9, and 6/9 ML. Thermodynamic analysis as given in Figures 7a–7h also shows that
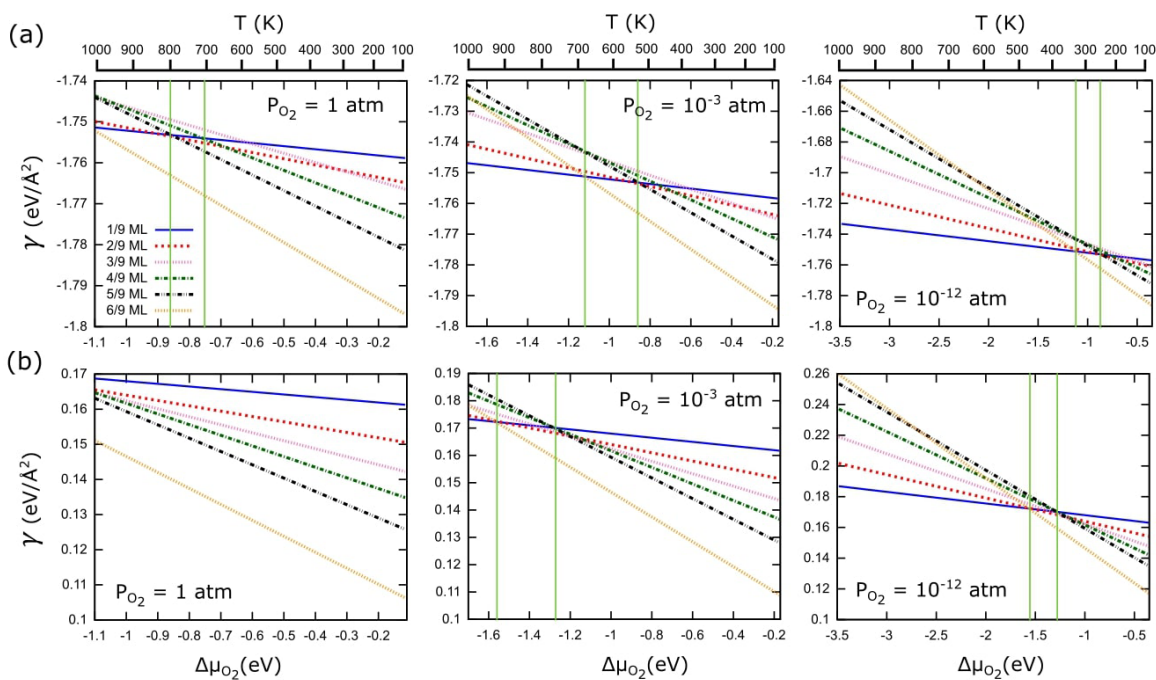
Figure 6. Surface free energy (γ) as a function of the chemical potential of oxygen (μ_{O_2}) for different on-surface O coverage depending on the temperature at a fixed partial pressure of O_2, $P_{O_2} = 1$, 10^{-3}, and 10^{-12} atm (or equivalently the corresponding temperature values at a fixed O_2 pressure) on (a) Au(211) and (b) AgAu(211) surfaces. The green vertical lines stands for the phase transition.

higher partial pressure of O_2 and lower temperature can stabilize the surface. We have found that, for the bare Au(211) surface, a coverage of 1/9 ML oxygen is the most thermodynamically stable above room temperature and 1 atm pressure, and 2/9 ML O becomes more stable around room temperature. When a Ag atom is substituted to the surface (see Figure 7b), the transition from the 1/9 ML to 2/9 ML O coverage occurs at higher temperature as a result of strong O-metal interaction (see Figures 7b–7e). While the 3/9, 4/9, and 5/9 ML Ag coverage can stabilize the surface at O coverage of 2/9 ML at lower chemical potential (or equivalently lower temperature), the trend changes at higher temperatures for the surface at O coverage of 3/9 ML; see Figures 7d–7f. It is easy to see that the 6/9 ML O coverage is obviously separated, and it is the most stable one on the AgAu(211) surface at the Ag coverage of 6/9 ML as seen in Figure 7g. Overall, the fully O-covered surface of AgAu(211) at different Ag coverages is the most stable at lower temperatures, and the phase transition from the higher O coverage to lower O coverage is only observed at higher temperature. It can be said that the O is thermodynamically stable at ambient thermodynamic conditions for the higher Ag concentration on the surface.

4. Summary and conclusion

We have presented an internally consistent thermodynamical approach for the calculation of the thermodynamic stability of transition metal surfaces. To establish a relationship between the calculations and experimental conditions, we have used this atomistic thermodynamic scheme for the O on flat Ag(111) and Au(111) and step Au(211) and bimetallic AgAu(211) surfaces. In order to assess the extent of surface oxidation in the presence of
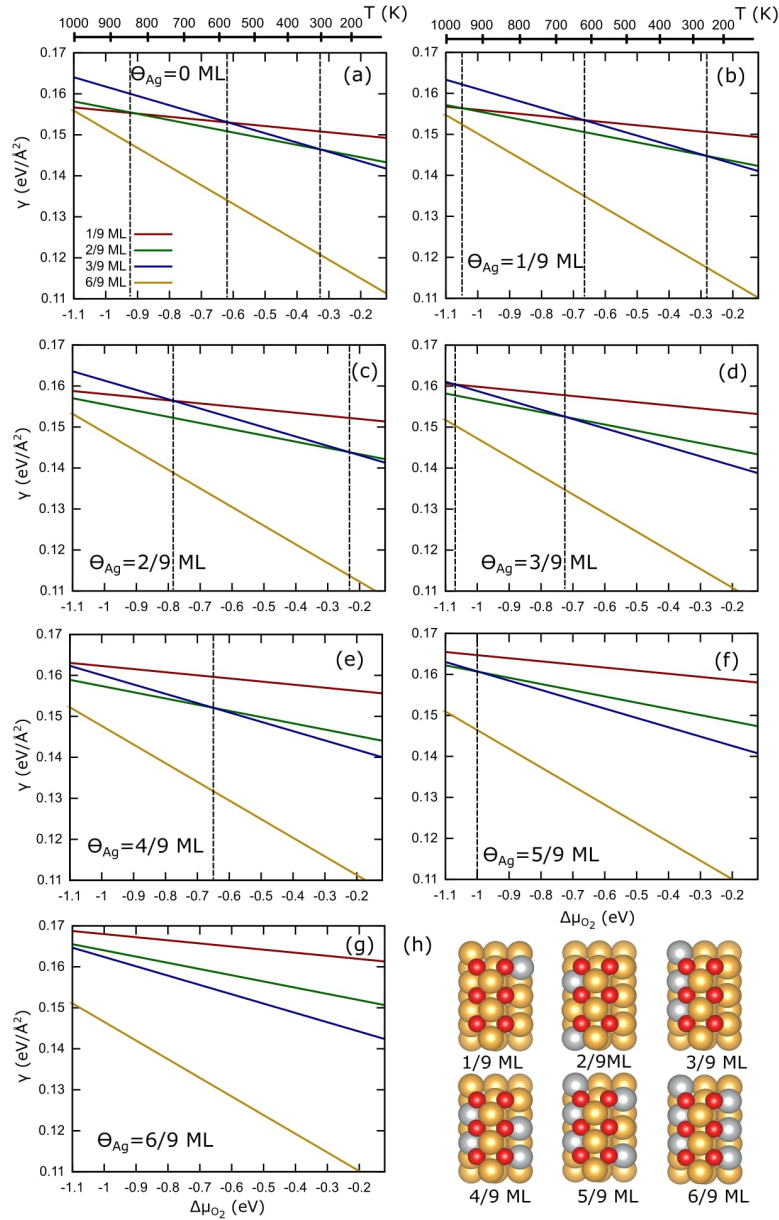
Figure 7. Surface free energy (γ) as a function of the chemical potential of oxygen ($\Delta\mu_{O_2}$) for the most stable structures with O coverage of 1/9, 2/9, 3/9, and 6/9 ML on AgAu(211) surface depending on the temperature at a fixed partial pressure of O_2, $P_{O_2} = 1$ atm. (a) Bare Au(211), (b)–(g) AgAu(211) with Ag coverage, Θ_{Ag}, in the range of 1/9 and 6/9 ML. Dashed vertical lines show the change of the thermodynamic stability of the surfaces. Gray, gold, and red balls stand for Ag, Au, and O, respectively.

ambient oxygen, several oxygen coverages are studied on the surfaces. We have found that the O atoms on the Ag(111) surface are more stable than the Au(111) surface with respect to the calculated adsorption energies. Besides this, the Ag atoms on the Au(111) surface lead to extra stabilization in the case of O adsorption. However, the subsurface Ag has little effect on isolated O in Au(111). The O stabilization on the surface decreases due to the repulsive interaction between the surface O atoms increasing the adsorption energies with

the increase of the O coverage. We have observed that 2/9 ML O coverage is the most stable O adsorption configuration on both flat surfaces. We have found that the O-O interactions are repulsive on the (111) surface, while the O-O interactions can be attractive on the (211) surface due to the formation of linear O-Au-O atomic arrangements.

In order to elucidate the temperature and pressure dependence of the adsorption of oxygen on the Ag(111), Au(111), Au(211), and AgAu(211) surfaces, we have used a DFT-based atomistic thermodynamic model. For the Ag(111) surface, O coverage lower than 4/9 ML is found to be the most stable at temperatures lower than 400 K. At higher O_2 partial pressure (1 atm), the 1/9 ML O coverage becomes the most stable one. Overall, the lower O coverages in Ag(111) are more stable at lower temperature and higher pressure. For the Au(111) and Au/Ag/Au(111) surfaces the surface free energy profiles are nearly same, and the most favorable O coverages are 1/9 and 2/9 ML O. However, the 3/9 ML O coverage on Ag/Au(111) is found to be stable at a wide range of temperatures and pressures, and the O may be observed under UHV conditions in the experiment. It is interesting to note that O coverages lower than 3/9 ML are more stable on Ag(111) surface. For the bimetallic AgAu(211) surface, the maximum surface O coverage is the most stable coverage at low temperatures and high pressures. Moreover, the oxygen is quite stable on the step at both low and high surface O coverage in AgAu(211). We have found that the Ag concentration can affect the thermodynamic stability of surface O, and the surface O at higher surface Ag concentration is stable at ambient thermodynamic conditions.

Acknowledgment

References

[1] Wittstock A, Biener J, Bäumer M. Nanoporous gold: a new material for catalytic and sensor applications. Physical Chemistry Chemical Physics 2010; 12: 12919-12930. doi: 10.1039/C0CP00757A.

[2] Moskaleva LV, Rohe S, Wittstock A, Zielasek V, Kluner T et al. Silver residues as a possible key to a remarkable oxidative catalytic activity of nanoporous gold. Physical Chemistry Chemical Physics 2011; 13: 4529-4539. doi: 10.1039/C0CP02372H.

[3] Stowers K, Madix R, Friend C. From model studies on Au(111) to working conditions with unsupported nanoporous gold catalysts: oxygen-assisted coupling reactions. Journal of Catalysis 2013; 308: 131-141. doi: 10.1016/j.jcat.2013.05.033.

[4] Wittstock A, Bäumer M. Catalysis by unsupported skeletal gold catalysts. Accounts of Chemical Research 2014; 47: 731-739. doi: 10.1021/ar400202p.

[5] Barakat T, Rooke JC, Genty E, Cousin R, Siffert S et al. Gold catalysts in environmental remediation and water-gas shift technologies. Energy and Environmental Science 2013; 6: 371-391. doi: 10.1039/C2EE22859A.

[6] Xu B, Madix RJ, Friend CM. Predicting gold-mediated catalytic oxidative-coupling reactions from single crystal studies. Accounts of Chemical Research 2014; 47: 761-772. doi: 10.1021/ar4002476.

[7] Burch R. Gold catalysts for pure hydrogen production in the water-gas shift reaction: activity, structure and reaction mechanism. Physical Chemistry Chemical Physics 2006; 8: 5483-5500. doi: 10.1039/B607837K.

[8] Samano E, Kim J, Koel BE. Investigation of CO oxidation transient kinetics on an oxygen pre-covered Au(211) stepped surface. Catalysis Letters 2009; 128: 263-267. doi: 10.1007/s10562-008-9815-8.

[9] Montemore MM, van Spronsen MA, Madix RJ, Friend CM. O_2 activation by metal surfaces: implications for bonding and reactivity on heterogeneous catalysts. Chemical Reviews 2018; 118: 2816-2862. doi: 10.1021/acs.chemrev.7b00217.

[10] Lefferts L, van Ommen J, Ross J. The oxidative dehydrogenation of methanol to formaldehyde over silver catalysts in relation to the oxygen-silver interaction. Applied Catalysis 1986; 23: 385-402. doi: 10.1016/S0166-9834(00)81306-8.

[11] Grabow LC, Hvolbæk B, Nørskov JK. Understanding trends in catalytic activity: the effect of adsorbate–adsorbate interactions for CO oxidation over transition metals. Topics in Catalysis 2010; 53: 298-310. doi: 10.1007/s11244-010-9455-2.

[12] Serafin J, Liu A, Seyedmonir S. Surface science and the silver-catalyzed epoxidation of ethylene: an industrial perspective. Journal of Molecular Catalysis A 1998; 131: 157-168. doi: 10.1016/S1381-1169(97)00263-X.

[13] Chatterjee D, Deutschmann O, Warnatz J. Detailed surface reaction mechanism in a three-way catalyst. Faraday Discussions 2002; 119: 371-384. doi: 10.1039/B101968F.

[14] Fajín JLC, Cordeiro MNDS, Gomes JRB. On the theoretical understanding of the unexpected O_2 activation by nanoporous gold. Chemical Communications 2011; 47: 8403-8405. doi: 10.1039/C1CC12166A.

[15] Ferrando R, Jellinek J, Johnston RL. Nanoalloys: From theory to applications of alloy clusters and nanoparticles. Chemical Reviews 2008; 108: 845-910. doi: 10.1021/cr040090g.

[16] Biener J, Biener MM, Madix RJ, Friend CM. Nanoporous gold: understanding the origin of the reactivity of a 21st century catalyst made by pre-Columbian technology. ACS Catalysis 2015; 5: 6263-6270. doi: 10.1021/acscatal.5b01586.

[17] Wittstock A, Wichmann A, Biener J, Bäumer M. Nanoporous gold: a new gold catalyst with tunable properties. Faraday Discussion 2011; 152: 87-98. doi: 10.1039/C1FD00022E.

[18] Déronzier T, Morfin F, Lomello M, Rousset JL. Catalysis on nanoporous gold-silver systems: Synergistic effects toward oxidation reactions and influence of the surface composition. Journal of Catalysis 2014; 311: 221-229. doi: 10.1016/j.jcat.2013.12.001.

[19] Montemore MM, Madix RJ, Kaxiras E. How does nanoporous gold dissociate molecular oxygen? Journal of Physical Chemistry C 2016; 120: 16636-16640. doi: 10.1021/acs.jpcc.6b03371.

[20] Zugic B, Wang L, Heine C, Zakharov DN, Lechner BAJ et al. Dynamic restructuring drives catalytic activity on nanoporous gold-silver alloy catalysts. Nature Materials 2016; 16: 558-564. doi: 10.1038/nmat4824.

[21] Fujita T, Guan P, McKenna K, Lang X, Hirata A et al. Atomic origins of the high catalytic activity of nanoporous gold. Nature Materials 2012; 1: 775-780. doi: 10.1038/nmat3391 DO - 10.1038/nmat3391 ID.

[22] Roldán A, González S, Ricart JM, Illas F. Critical size for O_2 dissociation by Au nanoparticles. Chemical Physics and Physical Chemistry 2009; 10: 348-351. doi: 10.1002/cphc.200800702.

[23] Kim J, Samano E, Koel BE. Oxygen adsorption and oxidation reactions on Au(211) surfaces: exposures using O_2 at high pressures and ozone (O_3) in UHV. Surface Science 2006; 600: 4622-4632. doi: 10.1016/j.susc.2006.07.057.

[24] Xinhe B, Jingfa D. The oxidation of methanol on electrolytic silver catalyst. Journal of Catalysis 1986; 99: 391-399. doi: 10.1016/0021-9517(86)90364-7.

[25] Waterhouse GI, Bowmaker GA, Metson JB. Mechanism and active sites for the partial oxidation of methanol to formaldehyde over an electrolytic silver catalyst. Applied Catalysis A 2004; 265: 85-101. doi: 10.1016/j.apcata.2004.01.016.

[26] Bao X, Muhler M, Pettinger B, Schlögl R, Ertl G. On the nature of the active state of silver during catalytic oxidation of methanol. Catalysis Letters 1993; 22: 215-225. doi: 10.1007/BF00810368.

[27] Nagy A, Mestl G, Rühle T, Weinberg G, Schlögl R. The dynamic restructuring of electrolytic silver during the formaldehyde synthesis reaction. Journal of Catalysis 1998; 179: 548-559. doi: 10.1006/jcat.1998.2240.

[28] Baker TA, Liu X, Friend CM. The mystery of gold's chemical activity: local bonding, morphology and reactivity of atomic oxygen. Physical Chemistry Chemical Physics 2011; 13: 34-46. doi: 10.1039/C0CP01514H.

[29] Quiller RG, Baker TA, Deng X, Colling ME, Min BK et al. Transient hydroxyl formation from water on oxygen-covered Au(111). Journal of Chemical Physics 2008; 129: 064702. doi: 10.1063/1.2965821.

[30] Karatok M, Vovk EI, Koc AV, Ozensoy E. Selective catalytic ammonia oxidation to nitrogen by atomic oxygen species on Ag(111). Journal of Physical Chemistry C 2017; 121: 22985-22994. doi: 10.1021/acs.jpcc.7b08291.

[31] Reuter K, Scheffler M. Composition, structure, and stability of $RuO_2(110)$ as a function of oxygen pressure. Physical Review B 2001; 65: 035406. doi: 10.1103/PhysRevB.65.035406.

[32] Moskaleva LV, Weiss T, Klüner T, Bäumer M. Chemisorbed oxygen on the Au(321) surface alloyed with silver: a first-principles investigation. Journal of Physical Chemistry C 2015; 119: 9215-9226. doi: 10.1021/jp511884k.

[33] Li WX, Stampfl C, Scheffler M. Why is a noble metal catalytically active? The role of the O-Ag interaction in the function of silver as an oxidation catalyst. Physical Review Letters 2003; 90: 256102. doi: 10.1103/PhysRevLett.90.256102.

[34] Li WX, Stampfl C, Scheffler M. Insights into the function of silver as an oxidation catalyst by ab initio atomistic thermodynamics. Physical Review B 2003; 68: 165412. doi: 10.1103/PhysRevB.68.165412.

[35] Fronzi M, Piccinin S, Delley B, Traversa E, Stampfl C. Water adsorption on the stoichiometric and reduced CeO2(111) surface: a first-principles investigation. Physical Chemistry Chemical Physics 2009; 11: 9188-9199. doi: 10.1039/B901831J.

[36] Jones TE, Rocha TCR, Knop-Gericke A, Stampfl C, Schlögl R et al. Thermodynamic and spectroscopic properties of oxygen on silver under an oxygen atmosphere. Physical Chemistry Chemical Physics 2015; 17: 9288-9312. doi: 10.1039/C5CP00342C.

[37] Reuter K, Stampf C, Scheffler M. Ab initio atomistic thermodynamics and statistical mechanics of surface properties and functions. In: Yip S (editor). Handbook of Materials Modeling. Berlin, Germany: Springer, 2005, pp. 149-194.

[38] Kresse G, Furthmüller J. Efficiency of ab-initio total energy calculations for metals and semiconductors using a plane-wave basis set. Computational Materials Science 1996; 6: 15-50. doi: 10.1016/0927-0256(96)00008-0.

[39] Kresse G, Hafner J. Ab initio molecular dynamics for liquid metals. Physical Review B 1993; 47: 558-561. doi: 10.1016/0022-3093(95)00355-X.

[40] Perdew JP, Burke K, Ernzerhof M. Generalized gradient approximation made simple. Physical Review Letters 1996; 77: 3865-3868. doi: 10.1103/PhysRevLett.77.3865.

[41] Blöchl PE. Projector augmented-wave method. Physical Review B 1994; 50: 17953-17979. doi: 10.1103/PhysRevB.50.17953.

[42] Kresse G, Joubert D. From ultrasoft pseudopotentials to the projector augmented-wave method. Physical Review B 1999; 59: 1758-1775. doi: 10.1103/PhysRevB.59.1758.

[43] Monkhorst HJ, Pack JD. Special points for Brillouin-zone integrations. Physical Review B 1976; 13: 5188-5192. doi: 10.1103/PhysRevB.13.5188.

[44] Tkatchenko A, Scheffler M. Accurate molecular van der Waals interactions from ground-state electron density and free-atom reference data. Physical Review Letters 2009; 102: 073005. doi: 10.1103/PhysRevLett.102.073005.

[45] Rogal J. Stability, composition and function of palladium surfaces in oxidizing environments: a first-principle statistical mechanics approach. PhD, Freie Universität Berlin, Berlin, Germany, 2006.

[46] Zangwill A. Physics at Surfaces. Cambridge, UK: Cambridge University Press, 1988.

[47] Xu Y, Mavrikakis M. Adsorption and dissociation of O_2 on gold surfaces: effect of steps and strain. Journal of Physical Chemistry B 2003; 107: 9298-9307. doi: 10.1021/jp034380x.

[48] Klyushin AY, Rocha TCR, Hävecker M, Knop-Gericke A, Schlögl R. A near ambient pressure XPS study of Au oxidation. Physical Chemistry Chemical Physics 2014; 16: 7881-7886. doi: 10.1039/C4CP00308J.

[49] Wittstock A, Zielasek V, Biener J, Friend CM, Bäumer M. Nanoporous gold catalysts for selective gas-phase oxidative coupling of methanol at low temperature. Science 2010; 327: 319-322. doi: 10.1126/science.1183591.

[50] Personick ML, Zugic B, Biener MM, Biener J, Madix RJ et al. Ozone-activated nanoporous gold: a stable and storable material for catalytic oxidation. ACS Catalysis 2015; 5: 4237-4241. 10.1021/acscatal.5b00330.